doi:10.1038/nature20148

Reorientation of Sputnik Planitia implies a subsurface ocean on Pluto

F. Nimmo[1], D. P. Hamilton[2], W. B. McKinnon[3], P. M. Schenk[4], R. P. Binzel[5], C. J. Bierson[1], R. A. Beyer[6], J. M. Moore[6], S. A. Stern[7], H. A. Weaver[8], C. B. Olkin[7], L. A. Young[7], K. E. Smith[6] & the New Horizons Geology, Geophysics & Imaging Theme Team*

The deep nitrogen-covered basin on Pluto, informally named Sputnik Planitia, is located very close to the longitude of Pluto's tidal axis[1] and may be an impact feature[2], by analogy with other large basins in the Solar System[3,4]. Reorientation[5–7] of Sputnik Planitia arising from tidal and rotational torques can explain the basin's present-day location, but requires the feature to be a positive gravity anomaly[7], despite its negative topography. Here we argue that if Sputnik Planitia did indeed form as a result of an impact and if Pluto possesses a subsurface ocean, the required positive gravity anomaly would naturally result because of shell thinning and ocean uplift, followed by later modest nitrogen deposition. Without a subsurface ocean, a positive gravity anomaly requires an implausibly thick nitrogen layer (exceeding 40 kilometres). To prolong the lifetime of such a subsurface ocean to the present day[8] and to maintain ocean uplift, a rigid, conductive water-ice shell is required. Because nitrogen deposition is latitude-dependent[9], nitrogen loading and reorientation may have exhibited complex feedbacks[7].

The Sputnik Planitia basin is 3.5 km below its surroundings (Fig. 1) and is filled with a convecting layer of nitrogen ice, thought to be about 3–10 km thick[10,11]. This structure would yield a strongly negative gravity anomaly (Extended Data Fig. 1a); to generate the present-day positive gravity anomaly either a much thicker nitrogen (N_2) layer or some other source of extra mass at depth would be required.

Stereo topography[1,2] suggests a present-day elliptical shape of 1,300 km × 900 km. The topography resembles that of other large degraded impact basins such as Hellas (on Mars)[3] or Caloris (on Mercury)[4] and includes a sharp rim (informally known as Cousteau Rupes) to the northeast[1]. The elevated topography beyond the basin rim might represent ejecta, but a distinct ejecta blanket is not visible in images[1], perhaps because of modification by Pluto's ongoing surface geological activity. The centre of the Sputnik Planitia ellipse is at about 175° E, 18° N, or about 400 km from the tidal axis. A point randomly placed on the surface has only a 5% chance of being this close or closer to either tidal axis.

If Sputnik Planitia formed during an impact then its initial depth d_0 was probably about 7 km (see Methods), on the basis of the depths of unrelaxed basins on Iapetus and the Moon[12], with uncertainties introduced by the low velocities of Pluto impactors[13]. The horizontal scale of Sputnik Planitia suggests that a thickness of tens of kilometres of ice was removed during impact, and that impact-driven uplift of an ice–ocean interface (if the ocean is present) probably occurred[14]. This uplift is important because it represents a large mass excess (Extended Data Fig. 1c). On the Moon a combination of impact-driven uplift of dense mantle material and later surface addition of lavas after the crust has cooled and strengthened results in impact basins showing a positive gravity anomaly[15–17]. We argue below that an analogous set of processes occurred at Sputnik Planitia.

If Sputnik Planitia represents a positive gravity anomaly, tidal and rotational torques will have reoriented it towards the tidal axis. The calculated reorientation is mainly equatorward (Fig. 1c) and depends on the amplitude of the positive gravity anomaly, parameterized by

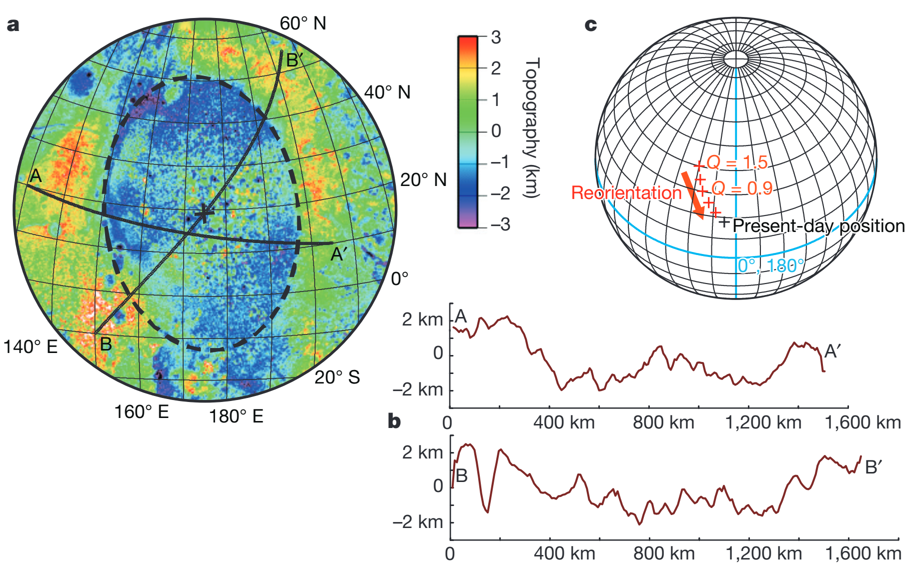

Figure 1 | Sputnik Planitia topography and reorientation. a, Stereo-derived topography of Sputnik Planitia (using method described in ref. 1) with an ellipse with axes 1,300 km × 900 km superimposed. The ellipse centre and projection centre (Lambert equal area) are both at 175° E, 18° N. **b**, Topographic profiles (locations shown in **a**). Point spacing was 8 km with 5-point averaging to reduce noise. **c**, Location of Sputnik Planitia before reorientation (red crosses) as a function of dimensionless gravity anomaly Q (in increments of 0.3). A Q value of 1.4 represents a nominal peak gravity anomaly Δg of +31 mGal (Methods) and yields about 20° true polar wander. Orthographic projection centred at 180° E, 45° N.

[1]Department of Earth and Planetary Sciences, University of California Santa Cruz, Santa Cruz, California 95064, USA. [2]Department of Astronomy, University of Maryland, College Park, Maryland 20742, USA. [3]Department of Earth and Planetary Sciences and McDonnell Center for the Space Sciences, Washington University in St Louis, St Louis, Missouri 63130, USA. [4]Lunar and Planetary Institute, Houston, Texas 77058, USA. [5]Department of Earth, Atmospheric and Planetary Sciences, Massachusetts Institute of Technology, Cambridge, Massachusetts 02139, USA. [6]National Aeronautics and Space Administration (NASA) Ames Research Center, Moffett Field, California 94035, USA. [7]Southwest Research Institute, Boulder, Colorado 80302, USA. [8]Johns Hopkins University Applied Physics Laboratory, Laurel, Maryland 20723, USA.
*A list of participants and their affiliations appears at the end of the paper.

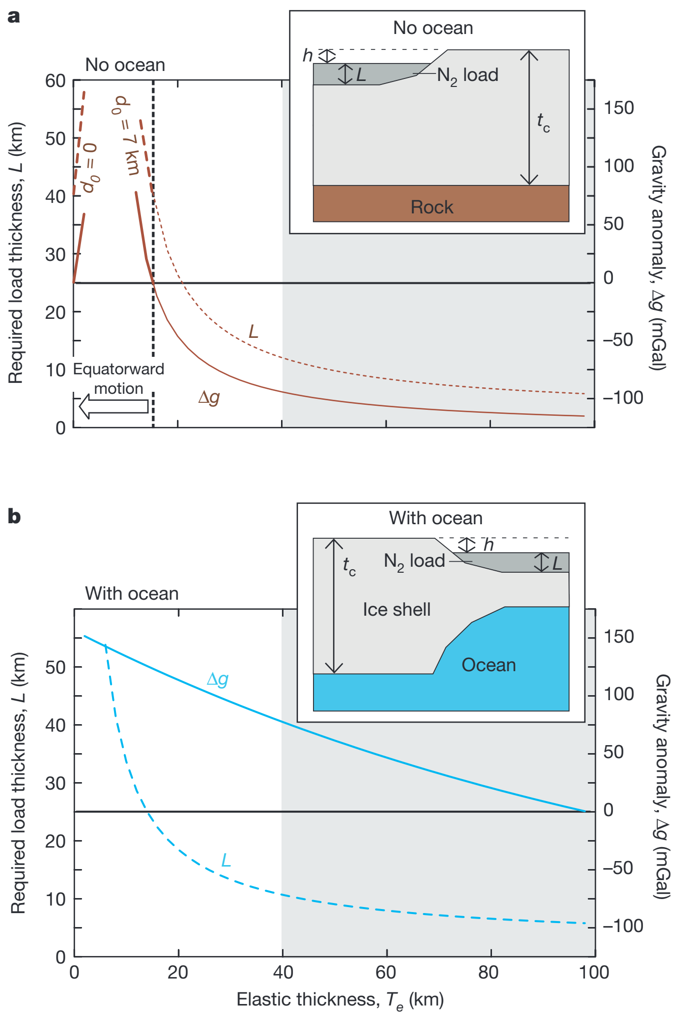

Figure 2 | Load thicknesses L and resulting gravity anomalies Δg for present-day Sputnik Planitia topography. **a**, Case with no ocean. Equatorward reorientation takes place if Δg is positive. Initial basin depth is d_0; to generate the present-day negative topography ($h = 3.5$ km) the deflection due to load thickness L is calculated using a thin-spherical-shell approach[30] (see Methods). The shaded region denotes the estimated elastic thickness range[18]. The characteristic wavenumber of Sputnik Planitia is taken to be $(4/3)\pi/D$, where D is the diameter (1,000 km). **b**, Case with ocean in which the pre-loading basin is isostatically compensated. Here $d_0 = 7$ km. The shell thickness t_c is taken to be $2T_e$ to calculate the gravity contribution of the water; this can be justified *a posteriori* by the requirement for a cold, conductive shell (Fig. 3). The insets show the model geometry assumed in each case.

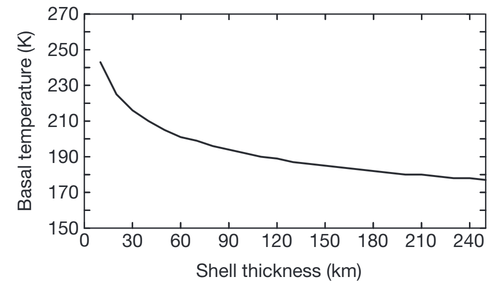

Figure 3 | Basal shell temperature required to maintain a thinned shell for 4 billion years. Timescale calculated using ref. 19 assuming a Newtonian viscosity of 10^{14} Pa s at 270 K and an activation energy of 50 kJ mol^{-1} (Methods). A conductive temperature profile was assumed with the surface at 40 K.

the dimensionless parameter Q (Methods). Because of Pluto's slow spin rate, the stabilizing effect of any remnant rotational bulge is small and equatorward reorientation can occur for modest (a few tens of milligals) positive gravity anomalies. A 20° reorientation increases the probability to 23% of Sputnik Planitia's initial location being as close to a tidal axis as it is observed to be. Our calculations are conservative because they neglect the role of the ejecta blanket, silicates contained in the impactor, and decoupling of the shell from the silicates underneath, all of which will serve to increase reorientation (Methods). Conversely, if Sputnik Planitia represents a present-day negative gravity anomaly it must have formed closer to the equator (Methods).

We now calculate likely gravity anomalies at Sputnik Planitia. If no ocean was present, uplift of the silicate interior is unlikely to have happened because of its rigidity and great depth[14] (assuming a differentiated body). In this case, we assume that deposition of N_2 of thickness L took place at a later epoch, by which time the crust had an elastic thickness T_e. Thermal evolution models predict that T_e always exceeds 40 km, depending mainly on when Sputnik Planitia formed[18]. Given d_0 and the present-day topography h, the load thickness L and the resulting gravity anomaly Δg can be calculated (Fig. 2a; Methods). For basins with initial depths in the range 0–7 km, positive gravity anomalies only occur with N_2 loads over 40 km thick and T_e values less than 15 km (so that the space required by the N_2 can be accommodated). A 40-km N_2 thickness is much larger than that inferred[10,11] and the T_e value is smaller than predicted[18]. The large negative gravity anomaly generated by the present-day 3.5-km negative topography is hard to overcome with N_2 loading alone.

If a subsurface ocean is present, the post-impact, pre-loading state is assumed to be isostatic, resulting in a thinned shell beneath the basin[14,16]. The dense water beneath the basin thus provides an additional positive contribution to the overall gravity. For example, Fig. 2b shows that in the presence of an ocean, an N_2 layer 7 km thick can generate a gravity anomaly of +32 mGal for $T_e = 70$ km. These values are consistent with the available constraints.

If Sputnik Planitia is a positive gravity anomaly at the present day, Fig. 2 suggests that a subsurface ocean with a thinned shell beneath the basin provides a viable explanation. Such a configuration will be smoothed out by lateral flow of the ice[19] at a rate dependent on the ice viscosity and the shell thickness t_c. Figure 3 shows that the configuration can be maintained for 4 billion years as long as the base of the ice shell is cold, that is, 180–250 K, depending on shell thickness. Such low temperatures can be achieved with an ocean containing ammonia and/or methanol[20] (ammonia is present in the Pluto system[21]) and imply a conductive shell, a large fraction of which will behave elastically. A conductive shell also transfers heat sufficiently slowly that a subsurface ocean can survive to the present day[8,22]. Preferential refreezing of the thinned portion of the shell could remove shell thickness contrasts. However, the thinned portion is capped by solid N_2, which has a much lower thermal conductivity than ice[23] and—even if convecting[10]—can provide sufficient insulation to prevent the thinned shell from refreezing (Methods).

Rather than uplift of liquid water underlying the ice shell, (1) uplift of mantle material, (2) dense, solid ice II, (3) silicate-rich ice or (4) reduced-porosity ice might instead be contributing to Δg. We argued above that the first possibility was unlikely. We do not favour the second alternative because the presence of ice II implies strongly compressional tectonics[20,22], for which there is no evidence[1]. Theoretical models[24] predict that silicate-rich ice, if present, should be found at the surface, because of the low temperatures, while deeper ice should be silicate-free. This is opposite to the required distribution. An impact-induced porosity reduction of 10% would need to extend to a depth of 70 km to compensate the basin, but for basins the size of Sputnik Planitia the porosity effect on gravity is probably overwhelmed by uplift of the underlying material[14,25]. Although impact-driven ocean uplift is expected for a Sputnik-Planitia-forming impact[14], further work will be required to exclude these other alternatives definitively.

An alternative hypothesis[26] suggests that the Sputnik Planitia basin formed by early loading of N_2 ice and reorientation as Pluto's spin state evolved to synchronous. In this hypothesis N_2 was subsequently removed from Sputnik Planitia; this removal would cause $>10°$ of polewards motion (Methods) and affect N_2 deposition. This prediction of polewards motion is opposite to that shown in Fig. 1; since reorientation[27] and load removal cause tectonic stresses, mapping of tectonic features[7] should be able to test which of these hypotheses is correct.

If Pluto contains a cold (probably ammonia-bearing) liquid ocean, several further issues arise. The predicted slow re-freezing of a Plutonian ocean results in isotropic extensional stresses[8,22], in agreement with the tectonic features observed[1]. The requirement for shell thinning to have occurred allows numerical models to probe the present-day shell thickness[14]. A rigid, conductive shell could be reconciled with putative cryovolcanic surface features[1] by appealing to ocean pressurization caused by progressive thickening of the ice shell[28]. Various Kuiper Belt Objects of somewhat similar sizes and densities (bulk compositions) to Pluto are known[29]; among these bodies, subsurface oceans are probably a common phenomenon.

Online Content Methods, along with any additional Extended Data display items and Source Data, are available in the online version of the paper; references unique to these sections appear only in the online paper.

Received 18 May; accepted 3 October 2016.
Published online 16 November 2016.

1. Moore, J. M. *et al.* The geology of Pluto and Charon through the eyes of New Horizons. *Science* **351,** 1284–1293 (2016).
2. Schenk, P.M. *et al.* A large impact origin for Sputnik Planum and surrounding terrains, Pluto? *Div. Planet. Sci. Meet.* **47,** abstr. 200.06 (2015).
3. Searls, M. L. *et al.* Utopia and Hellas basins, Mars: twins separated at birth. *J. Geophys. Res.* **111,** E08005 (2006).
4. Zuber, M. T. *et al.* Topography of the northern hemisphere of Mercury from MESSENGER laser altimetry. *Science* **336,** 217–220 (2012).
5. Rubincam, D. P. Polar wander on Triton and Pluto due to volatile migration. *Icarus* **163,** 469–478 (2003).
6. Nimmo, F. & Matsuyama, I. Reorientation of icy satellites by impact basins. *Geophys. Res. Lett.* **34,** L19203 (2007).
7. Keane, J. T., Matsuyama, I., Kamata, S. & Steckloff, J. K. Reorientation and faulting of Pluto due to volatile loading within Sputnik Planitia. *Nature* http://dx.doi.org/10.1038/nature20120 (2016).
8. Robuchon, G. & Nimmo, F. Thermal evolution of Pluto and implications for surface tectonics and a subsurface ocean. *Icarus* **216,** 426–439 (2011).
9. Binzel, R. P. *et al.* Climate zones on Pluto and Charon. *Icarus* http://dx.doi.org/10.1016/j.icarus.2016.07.023 (2016).
10. McKinnon, W. B. *et al.* Convection in a volatile nitrogen-ice-rich layer drives Pluto's geological and atmospheric vigour. *Nature* **534,** 82–85 (2016).
11. Trowbridge, A. J. *et al.* Vigorous convection as the explanation for Pluto's polygonal terrain. *Nature* **534,** 79–81 (2016).
12. White, O. L., Schenk, P. M. & Dombard, A. J. Impact basin relaxation on Rhea and Iapetus and relation to past heat flow. *Icarus* **223,** 699–709 (2013).
13. Bray, V. J. & Schenk, P. M. Pristine impact crater morphology on Pluto—expectations for New Horizons. *Icarus* **246,** 156–164 (2015).
14. Johnson, B. C., Bowling, T. J., Trowbridge, A. J. & Freed, A. M. Formation of the Sputnik Planum basin and the thickness of Pluto's subsurface ocean. *Geophys. Res. Lett.* **43,** 10068–10077 (2016).
15. Muller, P. M. & Sjogren, W. L. Mascons – lunar mass concentrations. *Science* **161,** 680–684 (1968).
16. Melosh, H. J. *et al.* The origin of lunar mascon basins. *Science* **340,** 1552–1555 (2013).
17. Wieczorek, M. A. & Phillips, R. J. Lunar multiring basins and the cratering process. *Icarus* **139,** 246–259 (1999).
18. Kamata, S. & Nimmo, F. Impact basin relaxation as a probe for the thermal history of Pluto. *J. Geophys. Res.* **119,** 2272–2289 (2014).
19. Nimmo, F. Non-Newtonian topographic relaxation on Europa. *Icarus* **168,** 205–208 (2004).
20. McKinnon, W. B., Simonelli, D. P. & Schubert, G. in *Pluto and Charon* (eds Stern, S. A. & Tholen, D. J.) 295–346 (Univ. Arizona Press, 1997).
21. Grundy, W. M. *et al.* Surface compositions across Pluto and Charon. *Science* **351,** aad9189 (2016).
22. Hammond, N. P., Barr, A. C. & Parmentier, E. M. Recent tectonic activity on Pluto driven by phase changes in the ice shell. *Geophys. Res. Lett.* **43,** 6775–6782 (2016).
23. Scott, T. A. Solid and liquid nitrogen. *Phys. Rep.* **27,** 89–157 (1976).
24. Rubin, M. E., Desch, S. J. & Neveu, M. The effect of Rayleigh-Taylor instabilities on the thickness of undifferentiated crust on Kuiper Belt Objects. *Icarus* **236,** 122–135 (2014).
25. Milbury, C. *et al.* Preimpact porosity controls the gravity signature of lunar craters. *Geophys. Res. Lett.* **42,** 9711–9716 (2015).
26. Hamilton, D. P. *et al.* The rapid formation of Sputnik Planitia early in Pluto's history. *Nature* http://dx.doi.org/10.1038/nature20586 (2016).
27. Matsuyama, I. & Nimmo, F. Rotational stability of tidally deformed planetary bodies. *J. Geophys. Res.* **112,** E11003 (2007).
28. Manga, M. & Wang, C.-Y. Pressurized oceans and the eruption of liquid water on Europa and Enceladus. *Geophys. Res. Lett.* **34,** L07202 (2007).
29. Brown, M. E. The compositions of Kuiper Belt Objects. *Annu. Rev. Earth Planet. Sci.* **40,** 467–494 (2012).
30. Turcotte, D. L. *et al.* Role of membrane stresses in the support of planetary topography. *J. Geophys. Res.* **86,** 3951–3959 (1981).

Acknowledgements New Horizons was built and operated by the Johns Hopkins Applied Physics Laboratory in Laurel, Maryland, USA, for NASA. We thank the many engineers, flight controllers and others who have contributed to the success of the New Horizons mission and NASA's Deep Space Network for a decade of excellent support to New Horizons. We thank B. Johnson for discussions on impact physics and J. Conrad for cryovolcanism calculations.

Author Contributions D.P.H. originated the reorientation hypothesis. F.N. developed the subsurface ocean scenario and carried out the bulk of the calculations. C.J.B. calculated the effect of realistic basin geometries and ejecta blanket. P.M.S. and R.A.B. provided the stereo topography. All authors read or commented on the manuscript.

Author Information Reprints and permissions information is available at www.nature.com/reprints. The authors declare no competing financial interests. Readers are welcome to comment on the online version of the paper. Correspondence and requests for materials should be addressed to F.N. (fnimmo@es.ucsc.edu).

Reviewer Information *Nature* thanks G. Collins and the other anonymous reviewer(s) for their contribution to the peer review of this work.

New Horizons Geology, Geophysics & Imaging Theme Team

J. M. Moore[1], W. B. McKinnon[2], J. R. Spencer[3], R. Beyer[1], R. P. Binzel[4], M. Buie[3], B. Buratti[5], A. Cheng[6], D. Cruikshank[1], C. Dalle Ore[1], A. Earle[4], R. Gladstone[7], W. Grundy[8], A. D. Howard[9], T. Lauer[10], I. Linscott[11], F. Nimmo[12], J. Parker[3], S. Porter[3], H. Reitsema[13], D. Reuter[14], J. H. Roberts[6], S. Robbins[3], P. M. Schenk[15], M. Showalter[16], K. Singer[3], D. Strobel[17], M. Summers[18], L. Tyler[11], O. L. White[1], O. M. Umurhan[1], M. Banks[19], O. Barnouin[6], V. Bray[20], B. Carcich[3], A. Chaikin[21], C. Chavez[1], C. Conrad[3], D. P. Hamilton[22], C. Howett[3], J. Hofgartner[23], J. Kammer[3], C. Lisse[6], A. Marcotte[6], A. Parker[3], K. Retherford[7], M. Saina[6], K. Runyon[5], E. Schindhelm[3], J. Stansberry[24], A. Steffl[3], T. Stryk[25], H. Throop[3], C. Tsang[3], A. Verbiscer[9], H. Winters[6], A. Zangari[3], S. A. Stern[3], H. A. Weaver[6], C. B. Olkin[3], L. A. Young[3] & K. E. Smith[1]

[1]National Aeronautics and Space Administration (NASA) Ames Research Center, Moffett Field, California 94035, USA. [2]Department of Earth and Planetary Sciences and McDonnell Center for the Space Sciences, Washington University in St Louis, Saint Louis, Missouri 63130, USA. [3]Southwest Research Institute, Boulder, Colorado 80302, USA. [4]Department of Earth, Atmospheric and Planetary Sciences, Massachusetts Institute of Technology, Cambridge, Massachusetts 02139, USA. [5]NASA Jet Propulsion Laboratory, Pasadena, California 91019, USA. [6]Johns Hopkins University Applied Physics Laboratory, Laurel, Maryland 20723, USA. [7]Southwest Research Institute, San Antonio, Texas 78238, USA. [8]Lowell Observatory, Flagstaff, Arizona 86001, USA. [9]University of Virginia, Charlottesville, Virginia 22904, USA. [10]National Optical Astronomy Observatory, Tucson, Arizona 85719, USA. [11]Stanford University, Stanford, California 94305, USA. [12]Department of Earth and Planetary Sciences, University of California Santa Cruz, Santa Cruz, California 95064, USA. [13]B612 Foundation, Mill Valley, California 94941, USA. [14]NASA Goddard Space Flight Center, Greenbelt, Maryland 20771, USA. [15]Lunar and Planetary Institute, Houston, Texas 77058, USA. [16]The SETI Institute, Mountain View, California 94043, USA. [17]The Johns Hopkins University, Baltimore, Maryland 21218, USA. [18]George Mason University, Fairfax, Virginia 22030, USA. [19]Planetary Science Institute, Tucson, Arizona 85719, USA. [20]University of Arizona, Tucson, Arizona 85721, USA. [21]Arlington, Vermont 05250, USA. [22]University of Maryland, College Park, Maryland 20742, USA. [23]Cornell University, Ithaca, New York 14853, USA. [24]Space Telescope Science Institute, Baltimore, Maryland 21218, USA. [25]Roane State Community College, Oak Ridge, Tennessee 37830, USA.

METHODS

Reorientation. To calculate the reorientation caused by Sputnik Planitia loading we follow the methods of ref. 27 with one exception. For a tidally distorted, slowly rotating synchronous satellite, the ratio of the non-normalized hydrostatic degree-two gravity coefficients is $J_2/C_{22} = 10/3$. However, since Pluto is the primary, it experiences less tidal distortion and the coefficient ratio is correspondingly higher, about 14.3 (ref. 7). As a result, we generalize equation (39) of ref. 27 as follows:

$$Q\sin 2\theta_L \cos(\phi_R - \phi_L) = \sin 2\theta_R \left(1 + \frac{f\cos^2\theta_T}{\sin^2\theta_R}\right) \quad (1)$$

Here Q is the dimensionless load size, θ and ϕ are colatitude and longitude, respectively, and the subscripts L, T and R refer to the final location of the load and the initial locations of the tidal axis and the rotational axis in the final reference frame. Here f is defined as $f = 3m/(M + m)$, where m and M are the masses of the tide-raising body (Charon) and Pluto, respectively, such that for a synchronous satellite orbiting a massive planet $f = 3$ (yielding equation (39) of ref. 27) while for a purely rotat ionally distorted body $f = 0$. With this modification the reorientation caused by an imposed load Q may be calculated. For simplicity, we assume that reorientation occurs as a single event, though in reality it may have consisted of progressive motion.

For $Q = 1$ and $f = 0.327$ (appropriate to Pluto) we find that $\theta_T = 102.5°$, $\phi_T = 193.1°$, $\theta_R = 13.6°$ (this is the amount of true polar wander, TPW) and $\phi_R = 169.6°$. A TPW of 20° requires $Q = 1.4$. The initial position of the load in the final reference frame may then be calculated using spherical triangles or by diagonalizing the moment of inertia tensor (ref. 27); for $Q = 1$ the load is initially located at 31.6° latitude and 163.2° longitude in the final reference frame.

A basin of constant depth h and angular radius ψ yields the following dimensionless load Q (ref. 6):

$$Q = \frac{3\pi G h \rho \cos\psi \sin^2\psi}{R\Omega^2 \Delta k_2} = \frac{3}{2}\frac{p\Delta g \cos\psi \sin^2\psi}{R\Omega^2 \Delta k_2} \quad (2)$$

where G is the gravitational constant, ρ is the density of the material, R and Ω are the radius and rotation angular frequency of Pluto and Δk_2 is the difference between the fluid Love number and the actual Love number (this quantity describes the size of the remnant bulge, which opposes reorientation). The numerator depends on the size of the load and the denominator represents the remnant bulge size. The size of the remnant bulge depends on Δk_2 and the rotation rate at which the bulge was 'frozen in'. Existing shape observations show no evidence of a remnant bulge[31] and the establishment of Pluto's present-day spin rate probably took a few million years[31], whereas cooling of the interior and freezing in of a remnant bulge probably took tens to hundreds of millions of years[8,22]. We therefore take the relevant rotation rate to be that of the present day. The second equality introduces the peak gravity anomaly Δg associated with the basin. For a parabolic basin (as we assume for Sputnik Planitia), the peak gravity is the same as for the constant-depth case, but the corresponding value of Q is reduced by a factor of $p \approx 0.5$ because the mean basin depth is smaller. We take $R = 1{,}188$ km, $p = 0.5$, $\Omega = 1.14 \times 10^{-5}$ rad s^{-1}, and $\psi = 24°$ ($D = 1{,}000$ km). For a Pluto with a 50-km-thick elastic lithosphere $\Delta k_2 = 0.16$ (see below) in which case equation (2) yields $\Delta g = 22Q$ mGal. A larger Δk_2 (larger remnant bulge) would require a larger gravity anomaly to get the same amount of reorientation.

Our calculated degree of reorientation is probably conservatively small, for three reasons. First, if present, an ejecta blanket will reduce the size of the original negative gravity anomaly associated with the basin (yielding $p \approx 0.3$). Second, the basin-forming impactor probably contained some silicates, so any impactor material incorporated into the ice shell will provide a positive contribution to gravity. Third, a decoupled ice shell is likely to reorient more than a solid body. However, for our argument the degree of reorientation is less important than the sign: only a basin exhibiting a positive gravity anomaly will experience equatorward reorientation.

Polewards motion. For a load near the tidal axis and for a body (like Pluto) that is primarily rotationally distorted, we can approximate equation (1) as $Q\sin 2\theta_L \approx \sin 2\theta_R$ with $\theta_L = 72°$ for present-day Sputnik Planitia. The present-day gravity anomaly in the absence of a subsurface ocean is about -115 mGal (Extended Data Fig. 1a). Using the present-day rotation period and setting $\Delta k_2 = 1$ to represent the largest likely remnant bulge (the real value is probably considerably smaller; see below) and with $\Delta g = -115$ mGal, equation (2) shows that the corresponding value of Q is -0.8. This in turn implies a poleward reorientation θ_R of about 14°, and an original (pre-reorientation) latitude of 4°. A smaller remnant bulge would result in more reorientation. If Sputnik Planitia is a negative gravity anomaly at the present day, or if mass was removed after its equilibrium position was established, Sputnik Planitia should have experienced large poleward reorientation, because the stabilizing effect of the rotational remnant bulge is small.

Loading calculations. Consider first a basin that is initially isostatically compensated by an uplifted root (the with-ocean case), so that the initial gravity anomaly is about zero. The initial uplift r is given by $r = d_0\rho_c/(\rho_m - \rho_c)$, where ρ_m and ρ_c are the density of water and ice, respectively, and d_0 is the depth of the basin after rebound. Assuming that an initially unstressed elastic layer develops after the rebound is complete, subsequent loading results in deflection. Taking the load thickness to be L, the deflection w (positive downwards) and the final basin negative topography h, we have

$$h = d_0 + w - L \quad (3)$$

For a load described by a single spherical harmonic degree n, the required load thickness L for a given h can then be obtained via

$$L = \frac{(h - d_0)(C'_n + 1)}{\left(\frac{\rho_L - \rho_c}{\rho_c}C'_n - 1\right)} \quad (4)$$

Here ρ_L is the load density, $C'_n = \frac{\rho_c}{\rho_m - \rho_c}C_n$ where C_n is the degree of compensation[30], which depends on the elastic thickness, and we have modified the definition from ref. 30 to avoid singularities arising when $\rho_m = \rho_c$. In the rigid limit there is no deflection, so $C'_n = 0$, and equation (4) yields the correct answer: $L = d_0 - h$. In the isostatic limit $C'_n = \frac{\rho_c}{\rho_m - \rho_c}$ and again the correct answer is recovered, yielding a much larger load thickness: $L = (d_0 - h)\rho_m/(\rho_m - \rho_L)$.

The post-loading peak gravity anomaly is given by

$$\Delta g = 2\pi G(-[h + L]\rho_c + L\rho_L + [r - w][\rho_w - \rho_c]e^{-kt_c}) \quad (5)$$

The final term in equation (5) represents the positive gravity contribution of the uplifted dense water. Here the factor $\exp(-kt_c)$ is due to upwards attenuation of the gravity anomaly owing to the finite shell thickness t_c. We take $t_c = 2T_e$.

Next we consider a basin overlying a flat ice–silicate interface (the no-ocean case). The depth after any initial (pre-loading) flexure is taken to be d_0. The required load thickness can again be obtained from equation (4), where in this case C'_n is calculated by setting $\rho_m = \rho_c$ (because there is no contribution from a higher-density layer at depth). Again, the correct answer is recovered in the rigid and isostatic limiting cases. In this case the peak gravity anomaly is then simply

$$\Delta g = 2\pi G(-[h + L]\rho_c + L\rho_L) \quad (6)$$

We calculate C_n using equation (27) of ref. 30. We convert from wavenumber k to spherical harmonic degree n by using $n \approx kR$. The Young's modulus of ice is 9 GPa, densities of water ice, water and N_2 ice are taken to be 0.92 g cm^{-3}, 1.0 g cm^{-3} and 1.0 g cm^{-3} (ref. 23), respectively. Incorporation of ammonia into the ice could in theory reduce its effective rigidity, but during slow freezing ammonia will be excluded from the crystallizing ice[32].

In reality, Sputnik Planitia loading consists of contributions from multiple wavenumbers. To determine the dominant wavenumber, we calculated the flexural deflection of a parabolic basin using the approach of ref. 33 and determined that the maximum deflection is well approximated by an effective wavenumber $k = 4\pi/3D$, where D is the basin diameter.

Lateral flow of the shell. The timescale for lateral flow of the shell is calculated using the approach of ref. 22, which gives the relaxation timescale τ:

$$\tau = \frac{\eta_b}{g\Delta\rho\delta^3 k^2}$$

where η_b is the basal viscosity, k is the wavenumber as before, δ is the effective layer thickness in which flow occurs and $\Delta\rho$ is the ice–water density contrast. The basal viscosity depends on the reference viscosity and the activation energy Q_a, and for a shell in which conductivity varies as $1/T$, δ is given by

$$\delta = \frac{R_g T_b t_c}{Q_a \ln(T_b/T_s)}$$

where R_g is the gas constant and T_b and T_s are the basal and surface temperatures.

Size of remnant bulge. The size of the remnant bulge[27,34] is assumed to depend on the quantity $k_{2f} - k_2$, where k_{2f} is the Love number after all stresses have relaxed and k_2 is the present-day Love number. A body which is fluid at the present day has no remnant bulge ($k_{2f} - k_2 = 0$) while a body which is infinitely rigid now ($k_2 = 0$) has the largest possible remnant bulge, the size of which depends on the density structure and initial rotation rate. We use the method of ref. 35 to calculate the Love numbers and assume that the body is spherically symmetric. We assume that Pluto's silicate interior has remained rigid and unrelaxed at all timescales and has an outer radius of 842 km, a rigidity of 100 GPa and a density of 3.5 g cm^{-3}. The overlying H_2O layer has a mean density of 0.95 g cm^{-3} and an outer radius of 1,188 km. In the presence of an elastic ice shell 50 km thick with a shear modulus of 3 GPa, $k_2 = 0.28$, while in the absence of such a shell $k_{2f} = 0.44$. The fact that $(k_{2f} - k_2) \approx k_2$ implies that the remnant bulge and present-day bulge are of comparable magnitude. Our assumption of a rigid silicate core is based on thermal evolution calculations[8]; if the core were instead strengthless at all timescales, the Love numbers increase to $k_2 = 0.52$ and $k_{2f} = 0.75$, respectively.

Initial depth of Sputnik Planitia basin. Pluto's radius is close to the geometric mean of the radii of Iapetus ($R = 734$ km) and the Moon ($R = 1,738$ km). Basins a thousand kilometres across that appear to be unrelaxed exist on Iapetus and the Moon[12], with Iapetus basins approaching 10 km in depth and lunar basins about a factor of two shallower. A similar-scale unrelaxed basin on Pluto might therefore be expected to be about 7 km deep. The corresponding isostatic ocean uplift would be 80 km. Expected impact velocities on Pluto are lower even than on Iapetus, but the implications of these lower velocities for the initial depth-to-diameter ratio of the resulting basin are unclear[13].

The extent to which crust (shell) thinning and mantle (ocean) uplift occur in response to an impact depend on the diameter of the basin relative to the depth to the mantle, or ocean[14,16]. On the Moon, with a mean crustal thickness of about 35 km, mantle uplift occurs for basins with diameters in excess of 220 km (refs 25 and 36). Assuming that this same ratio applies to Pluto, a 1,000-km-diameter basin would be expected to generate ocean uplift for shells thinner than about 160 km. This expectation is confirmed by numerical models[14], which show that uplift occurs for ice-shell thicknesses less than about 180 km. A chondritic Pluto might have a present-day shell thickness similar to this value[8,24], while in the past the shell will have been thinner and uplift will correspondingly be more likely to have occurred.

Insulating effect of N_2. Consider a reference shell of thickness t_c and effective thermal conductivity k_c. It may be compared with a thinned shell of total thickness t_c' containing a layer of lower-conductivity ice k' of thickness L. For the heat fluxes across the two shells to be equal, the required thickness of the insulating ice L can be shown to be

$$L = \frac{k'}{k_c - k'}(t_c - t_c')$$

We note that this analysis neglects any melting at the base of the N_2 layer. Water ice exhibits a temperature-dependent thermal conductivity given by $651/T$ (ref. 37). The effective thermal conductivity k_c over the temperature range 40–240 K is then 5.8 W m^{-1} K^{-1}. In contrast, nitrogen ice at 50 K has a thermal conductivity of 0.2 W m^{-1} K^{-1} (ref. 23). The effective thermal conductivity of the nitrogen will be increased if it is convecting. Based on the results of ref. 10, the Nusselt number of the convecting nitrogen is about 3, so that the effective nitrogen thermal conductivity $k' \approx 0.6$ W m^{-1} K^{-1}.

For an initial basin depth of 7 km, the shell thinning after loading $(t_c - t_c')$ at Sputnik Planitia will be about 70 km, depending on the exact densities assumed and the amount of deformation. Thus, a nitrogen layer 8 km thick is sufficient to offset the increased heat flux due to the thinned shell. As a result, shell thickness variations can be maintained over geological timescales as long as an insulating N_2 ice layer persists. As shown in Fig. 2, a layer this thick will yield a positive gravity anomaly of about +30 mGal, sufficient to cause reorientation.

Code availability. Codes for the reorientation, loading and lateral flow calculations are available upon request from F.N.

31. Nimmo, F. *et al.* Mean radius and shape of Pluto and Charon from New Horizons images. *Icarus* http://dx.doi.org/10.1016/j.icarus.2016.06.027 (2016).
32. Kargel, J. S. Ammonia water volcanism on icy satellites—phase relations at 1-atmosphere. *Icarus* **100,** 556–574 (1992).
33. Comer, R. P., Solomon, S. C. & Head, J. W. Mars—thickness of the lithosphere from the tectonic response to volcanic loads. *Rev. Geophys.* **23,** 61–92 (1985).
34. Willemann, R. J. Reorientation of planets with elastic lithospheres. *Icarus* **60,** 701–709 (1984).
35. Moore, W. B. & Schubert, G. The tidal response of Europa. *Icarus* **147,** 317–319 (2000).
36. Soderblom, J. M. *et al.* The fractured Moon: production and saturation of porosity in the lunar highlands from impact cratering. *Geophys. Res. Lett.* **42,** 6939–6944 (2015).
37. Petrenko, V. F. & Whitworth, R. W. *Physics of Ice* (Clarendon Press, 1999).

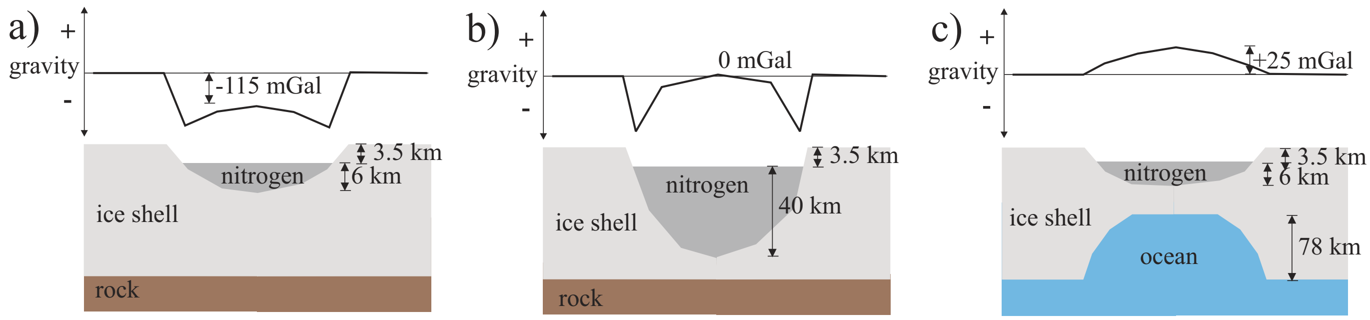

Extended Data Figure 1 | Schematic of the way in which the gravity anomaly is affected by an uplifted ocean and the thickness of the nitrogen layer. a–c, Either a nitrogen layer more than 40 km thick (**b**) or an uplifted ocean (**c**) could result in the present-day positive gravity anomaly at Sputnik Planitia; if neither is present, then a negative gravity anomaly results (**a**). The peak gravity anomaly is calculated using the flat-plate formula $2\pi G \Delta\rho h$ for each layer, where h represents the thickness, $\Delta\rho$ is the lateral density contrast and the densities of H_2O ice, water and N_2 ice are 0.92 g cm^{-3}, 1.0 g cm^{-3} and 1.0 g cm^{-3} (ref. 23), respectively. In **c**, the gravitational contribution of the ocean is reduced as a result of upwards attenuation assuming a shell thickness of 150 km (see Methods). The structure in **c** is similar to the inferred structure of lunar mascon basins, which also show positive gravity anomalies (refs 15, 16).